Detailed Multitechnique Spectroscopic Surface and Bulk Characterization of Plasma Polymers Deposited from 1-Propanol, Allyl Alcohol, and Propargyl Alcohol

F. FALLY,* I. VIRLET, J. RIGA, and J. J. VERBIST

Laboratoire Interdisciplinaire de Spectroscopie Electronique, Facultés Universitaires Notre-Dame de la Paix, Rue de Bruxelles, 61, B-5000 Namur, Belgium

SYNOPSIS

Three monomers with different degrees of unsaturation, 1-propanol, allyl alcohol, and propargyl alcohol, are plasma-deposited to obtain alcohol functions containing polymers. To obtain information on the behaviors of these monomers in the plasma, the polymers deposited in the reactor and in the postdischarge region are characterized by high-energy resolution XPS, IR, HREELS, elemental analysis, and chemical derivatization. XPS results show that oxygen-rich polymers can be obtained from the unsaturated monomers at low power for both regions or at high power in the postdischarge region. In the reactor at high power, fragmentation of the monomer leads to the elimination of oxygen fragments and ablation reactions during the polymerization process. Detailed structural information on the chemical structure and content of functional groups are obtained by simulation of the XPS C1s core levels of the polymers before and after derivatization with trifluoroacetic anhydride. In soft conditions, allyl alcohol leads to the formation of polymers with a relatively low degree of crosslinking and a high hydroxyl content (53–72%). However, the high resolution of the XPS spectrometer allows one to detect the presence of secondary or tertiary alcohol functions resulting from chain branching reactions in this polymer. Results from this multitechnique characterization indicate also that the hydroxyl conversion and crosslinking reactions are more pronounced for poly(1-propanol) and poly(propargyl alcohol). Alcohol, ether, and carbonyl functions are present in equivalent quantities in poly(propargyl alcohol) while poly(1-propanol) contains mainly ether functions (50%). The presence or absence of alcohol functions at the extreme surface of the polymers in relation to the chain mobility and the tendency of hydrogen bonding between hydroxyl groups was studied by HREELS. © 1996 John Wiley & Sons, Inc.

INTRODUCTION

Plasma deposition of monomers containing alcohol functions can be used to prepare hydrophilic thin films on solid substrates.[1] Moreover, alcohol functions at the surface of materials can serve for further modification: They can react with different reagents to immobilize useful functionalities. For example, postreactions of the hydroxylated surfaces with organosilane can be used to bind covalently amine-terminated siloxane monolayers.[2] Amine-terminated poly(ethylene oxide) can also be coupled to the hydroxylated surfaces.[3]

This could be a very good way to introduce primary amine functions at the surface of various materials. We have previously shown the difficulty to obtain directly primary amine functions by plasma polymerization of monomers containing amine functions (propylamine, allylamine, and propargylamine).[4] The proportion of primary amine functions in the plasma deposits was lower than 33%: These groups were converted into imine or nitrile functions in the discharge. The yield of primary amine functions introduced at the surface of polymers by NH_3 plasma treatment is also observed to be relatively low.[5]

* To whom correspondence should be addressed.

Journal of Applied Polymer Science, Vol. 59, 1569–1584 (1996)
 CCC 0021-8995/96/101569-16

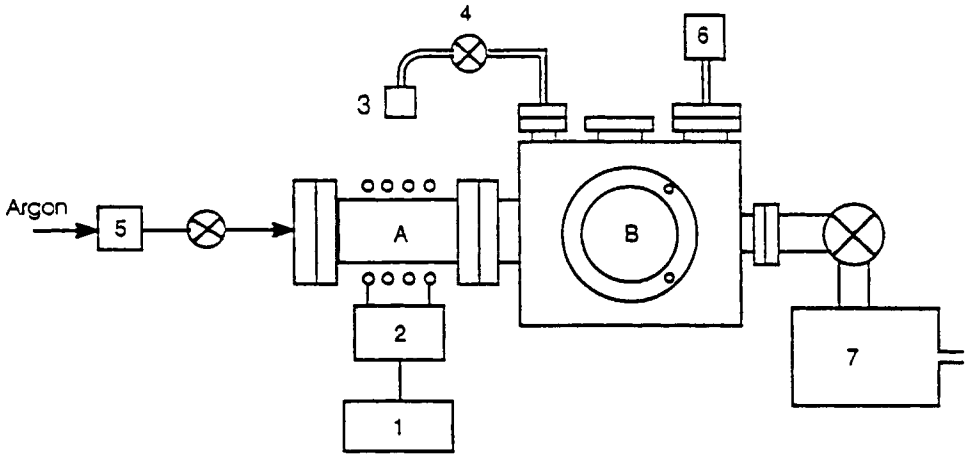

Figure 1 Apparatus for plasma polymerization: (1) rf power; (2) matching network; (3) monomer; (4) needle valve; (5) mass flow controller; (6) capacitance manometer; (7) pumping unit.

The alcohol functions can also be used to anchor chemically a Ziegler–Natta catalyst at the surface of a material.[6] This catalyst would then allow one to initiate polymerization processes at surfaces. Finally, hydroxylation of surfaces is also of interest in the field of biomaterials. For example, peptide sequences can be bonded covalently by reaction with the alcohol functions.[7]

However, it is well known that important fragmentation reactions leading to the elimination of oxygen-containing fragments occur during the polymerization of oxygen-containing monomers.[8–11] To minimize the loss of oxygen as well as the transformation of the hydroxyl group in the plasma, unsaturated monomers such as allyl alcohol (CH_2=CH—CH_2—OH) and propargyl alcohol (CH≡C—CH_2—OH) have been deposited under low-power conditions. We have previously shown that for these monomers the unsaturated carbon–carbon bonds are involved in the polymerization process, reducing thereby the fragmentation reactions.[12] Oxygen-rich films for which the proportion of the different functions have been determined could be polymerized.[12] To obtain more information on the polymerization mechanism, these plasma polymers are compared with the deposits formed from the corresponding saturated monomer (1-propanol, CH_3—CH_2—CH_2—OH).

Detailed structural information on the polymers is obtained by XPS, using a Scienta ESCA 300 spectrometer.[13] This spectrometer with high intensity and high-energy resolution provides quantitative chemical information on the plasma polymers. The percentage of alcohol functions is estimated by derivatization with trifluoroacetic anhydride (TFAA) in the vapor phase.[8,14] The hydrogen percentages are determined by elemental analysis for poly(propargyl alcohol). Quantitative information on the functional groups present in the polymers are compared with qualitative data obtained by transmission infrared spectroscopy (TIR) and high-resolution electron energy loss spectroscopy (HREELS).

EXPERIMENTAL

Chemicals

Propargyl alcohol and trifluoroacetic anhydride (TFAA) of 99% purity were obtained from Janssen. 1-Propanol (99%) and allyl alcohol (99%) were from Aldrich. Au-coated silicon wafers were used as substrates for the deposition and for the XPS and HREELS analysis, whereas KBr windows from Analis were used for infrared measurements.

Films Deposition

Polymers were deposited in an inductively coupled plasma reactor (Fig. 1). To compare the films formed from the three precursors at various powers, the other reactions conditions were kept invariant. After a stable argon flow rate was established (230 $cm^3_{(STP)}$/min), the monomer was introduced in the postdischarge region through a needle valve and polymerized with an rf power adjusted between 10 and 60 W. The total pressure in the plasma chamber during the polymerization was kept at 250 mTorr and the flow rates of the monomers were, respectively, 30, 37, and 20 $cm^3_{(STP)}$/min for 1-propanol, allyl alcohol, and propargyl alcohol.

Plasma polymer films were deposited on KBr windows for IR measurements. To minimize the charging effect, conducting silicon wafers covered with gold were used for the XPS and HREELS analysis. We compared the structure of the polymers deposited on substrates placed in the reactor (A) and in the postdischarge region (B).

To minimize the oxidation of the polymers upon air exposure, the reactor was brought back to atmospheric pressure via argon. The films were analyzed by XPS, IR, and HREELS directly (time exposure to the atmosphere lower than 2 min) after film preparation. The elemental analysis were only performed 2 months after deposition.

Film Characterization

X-ray photoelectron spectra were recorded on a Scienta ESCA 300 spectrometer using a high-power rotating anode (4100 rpm) and the monochromatized X-ray AlKα radiation (1486.7 eV). The spectrometer was operating at 0.75 mm slit width and 75 eV pass energy, giving an instrument resolution of 0.25 eV. The X-ray source was run at a power of 2 kW and charge compensation was achieved by the use of a low-energy electron gun. The polymers were analyzed at a 35° takeoff angle and the core levels were calibrated by reference to the first component of the C1s core level peak (unfunctionalized hydrocarbons) set at 285.0 eV.

The high-resolution XPS C1s and O1s core level spectra were resolved into individual peaks using a nonlinear least-square fitting program. The individual components were taken as a linear combination of a Lorentzian (10%) and a Gaussian (90%) curve. A shirley background was used to represent the contribution of the secondary electrons.

The content of alcohol functions in the films was determined by performing derivatization reactions with trifluoroacetic anhydride (TFAA). This labeling of the hydroxyl groups with fluorine was achieved by exposing the polymers to TFAA vapors for 15 min at 35°C.[8]

The thickness of the films deposited on gold substrates is estimated by XPS considering the dependence of the electron mean free path on kinetic energy. For higher energy than 150 eV, the electron mean free path increases as kinetic energy increases, $\lambda = BE^{1/2}$.[15] Hence, electrons from different gold energy levels have different escape depths from the sample surface. By comparison of the intensities of peaks from different gold energy levels (Au $4d_{5/2}$ and Au $4f_{7/2}$), an estimate of the overlayer thickness was obtained by using the equation described in Ref. 16.

A Perkin-Elmer 983G infrared spectrometer was used to collect transmission spectra of the films deposited on KBr windows.

The elemental compositions of the films were analyzed with a Heraeus CHN — O — Rapid elemental analyzer in the Central Research Laboratory from Solvay. Only films deposited from propargyl alcohol could be removed from large-size quartz substrates to give enough product for this type of analysis. The deposits were very adherent to the substrate. However, after immersion in water, swelling of the polymers occurred, so that they could easily be removed from the quartz substrate and transformed into powder upon drying *in vacuo*.

The HREEL spectra were recorded with a commercial spectrometer (SEDRA from Riber-ISA) consisting of two electrostatic deflectors, used as an electron monochromator and analyzer, respectively.[17] The primary electron beam had a kinetic energy of 5.2 eV and the recording specular geometry was at 45° from the normal for both incident and scattered beams. To minimize the charging effect, relatively thin films (around 100 Å) were deposited on conducting substrates (gold-covered silicon plates).

RESULTS AND DISCUSSION

XPS Characterization

Atomic Ratios

XPS results obtained from plasma polymerized 1-propanol show that the plasma polymerization of this saturated monomer leads to the formation of oxygen-deficient films (Fig. 2). In the reactor, for higher-power values than 12 W, thin films with O/C (×100) ratios lower than 8 were obtained. These polymer layers grow relatively slowly ($\cong$ 0.2 Å/s). Films of poly(1-propanol) with the higher oxygen content [O/C (×100) = 20] were obtained at 12 W in the reactor. In these conditions, the measured deposition rate is very low: $2.0 \cdot 10^{-2}$ Å/s. Because of still lower deposition rates (around 10^{-3} Å/s) in the postdischarge region, samples obtained from this monomer in the postdischarge region were not analyzed by XPS.

To obtain oxygen-rich polymers, unsaturated monomers must be deposited under well-defined conditions. The atomic ratios obtained from plasma-polymerized allyl alcohol and propargyl alcohol show strong variations. Under low-power conditions, oxygen-rich deposits are obtained in the postdischarge region and in the reactor (Fig. 2). The oxygen con-

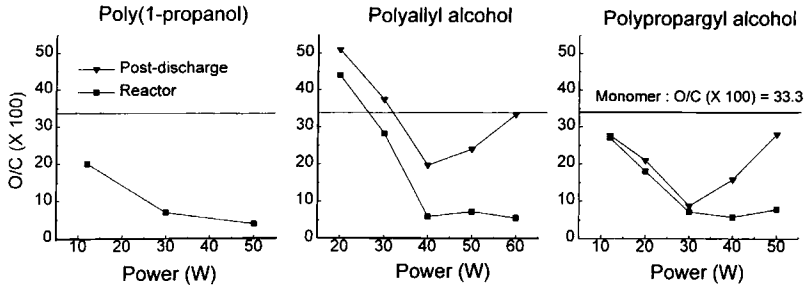

Figure 2 O/C ratios (×100) of the polymers obtained at different values of rf power.

tent is somewhat higher for films deposited in the postdischarge region.

For the unsaturated monomers, the oxygen content in the polymers decreases drastically as a function of power up to 40 W for polyallyl alcohol and up to 30 W for poly(propargyl alcohol). However, for higher-power conditions, the quantity of oxygen strongly depends on the sample position. In the postdischarge region, oxygen-rich polymers are again obtained, whereas the O/C ratio remains low for the samples located in the reactor. In both cases, allyl alcohol produces plasma polymers with a higher oxygen content than that of propargyl alcohol and the O/C ratio is always higher for the postdischarge position.

Two hypotheses can be proposed to explain these opposite evolutions of the oxygen content vs. power for the two sample positions: For high-energy input, the important electron temperature and electron density in the plasma[18] lead to a large degree of fragmentation of the monomer. It is possible that some oxygen-containing fragments relatively stable do not react directly in the reactor. These species could then react on their way to the pump. So, more oxygen would be fixed on substrates placed in the postdischarge region. The other explanation could be that the polymerization mechanism at high power in the postdischarge region is similar to that occurring in the reactor at low power. Actually, the low electron temperature and electron density in the plasma at low power or at high power in the postdischarge region would allow the polymerization to proceed with less fragmentation of the monomer. It is also possible that both phenomena mentioned above are involved.

Deposition Rates

Comparison of the deposition rates of the three monomers indicates that the unsaturated carbon–carbon bonds are involved in the polymerization process (Fig. 3). The deposition rate of 1-propanol in the reactor is very low: $2.0 \cdot 10^{-2}$ Å/s at 12 W and around 0.2 Å/s for higher-power values. Figure 3 shows that higher deposition rates are observed for the unsaturated monomers: Propargyl alcohol polymerizes more rapidly than does allyl alcohol which has a higher deposition rate than has the saturated monomer. Thicker films are also obtained on substrates placed in the reactor where the electron temperature and electron density are more important.

For the unsaturated monomers, an increase in deposition rate vs. power is observed to be followed by a drastic decrease. This evolution is characteristic of a competition between ablation and polymerization.[19] At low power, the reactions leading to the formation of a polymer predominate on the ablation reactions. By increasing the power, more radicals are created in the plasma. This contributes to the increase of the deposition rate. For higher-power values in the reactor, important fragmentation re-

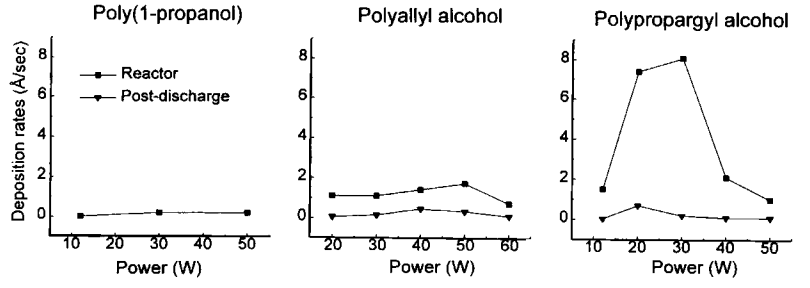

Figure 3 Deposition rates (Å/s) of the polymers obtained at different values of rf power.

actions of the monomer lead to the elimination of oxygen-containing fragments. These species are responsible for ablation.

This particular evolution of the deposition rates for the unsaturated monomers can be correlated to the atomic ratios. The decrease in deposition rate vs. power occurs at power values at which important elimination of oxygen fragments takes place in the reactor: For power values higher than 40 W for poly(allyl alcohol) and 30 W for poly(propargyl alcohol), O/C ratios (×100) between 6 and 8 were found in the deposits.

Evolution of the C1s Core Level Spectra

The evolution of the C1s core level spectra of poly(allyl alcohol) with power is shown in Figure 4. Due to the high-energy resolution of the Scienta ESCA 300 spectrometer, three components are well separated. The intensity of component B decreases vs. power for the films deposited in the reactor. On the other hand, for the postdischarge position, increasing the power gives rise to a decrease of B intensity up to 40 W followed by an increase at higher-power values.

Simulation of the C1s Core Levels

The simulation of the C1s core level spectra provides quantitative information on the oxygen functional groups in the polymer structure (Fig. 5). Four components are needed for simulating the spectra. The first one, due to carbon atoms in a CH_x environment (unfunctionalized carbon atoms), was positioned at 285.0 eV (A). The second component (B) located at 286.4 eV is due to carbon atoms single-bonded to oxygen (alcohol functions, ether functions, or epoxide groups), while the third component (C), at 287.8 eV, arises from carbonyl functions. The last component (D) (289.0 eV), of negligible intensity (lower than 1%), corresponds to carbon atoms from ester or carboxylic acid functions.

For poly(allyl alcohol), component C is relatively low compared to component B (Fig. 6). The percentage of component B and the atomic ratios follows a similar evolution vs. power. For oxygen-rich deposits of poly(allyl alcohol), the atomic ratio O/C (×100) reflects the percentage of carbon atoms bonded to oxygen (B + C) (Table I). It seems, therefore, that component B originates mainly from carbon atoms bonded to alcohol functions. The presence of ether functions or epoxide groups would give a higher oxygenated carbon percentage than the O/C ratio.

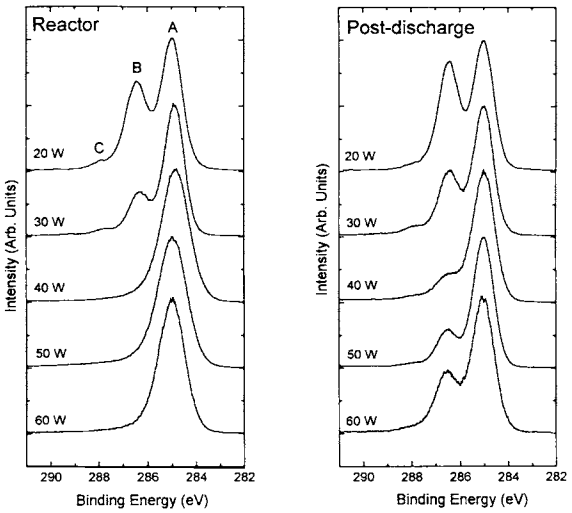

Figure 4 XPS C1s core levels spectra of poly(allyl alcohol).

The tendency to produce films with a great amount of alcohol functions is not so great in the case of 1-propanol and propargyl alcohol. From Table I, it seems that the B component is still due to alcohol functions for poly(propargyl alcohol), while for poly(propyl alcohol) obtained at 12 W, the higher percentage of carbon bonded to oxygen (B + C) than the O/C (×100) ratio is an indication of the presence of ether functions or epoxide groups. Figure 6 shows that, compared to poly(allyl alcohol), for low-power values, the percentage of B is smaller and that some more carbonyl functions are formed in these two polymers (higher percentage of C). This is also confirmed by the comparison of the O1s core levels spectra of the three polymers (Fig. 7). In the case of poly(allyl alcohol), the full-width at half-maximum (fwhm) is 1.2 eV and the binding energy corresponds to that of alcohol functions (532.8 eV). Larger fwhm (1.7–1.8 eV) are observed for poly(1-propanol) and poly(propargyl alcohol). These broader peaks are due to the presence of different oxygen-containing functionalities.

The comparison of the fwhm of component A resulting from the simulation of the C1s core levels gives additional information on the chemical structure of the polymers (Table II). For poly(allyl alcohol) deposited in the reactor at low power (20 and 30 W), relatively low fwhm (around 1.0 eV) are observed. These fwhm are close to those of the first component of the XPS C1s core level of conventional polymers such as poly(vinyl methyl ether), poly(propylene glycol), and poly(vinyl alcohol) analyzed in the same conditions (pass energy: 75 eV,

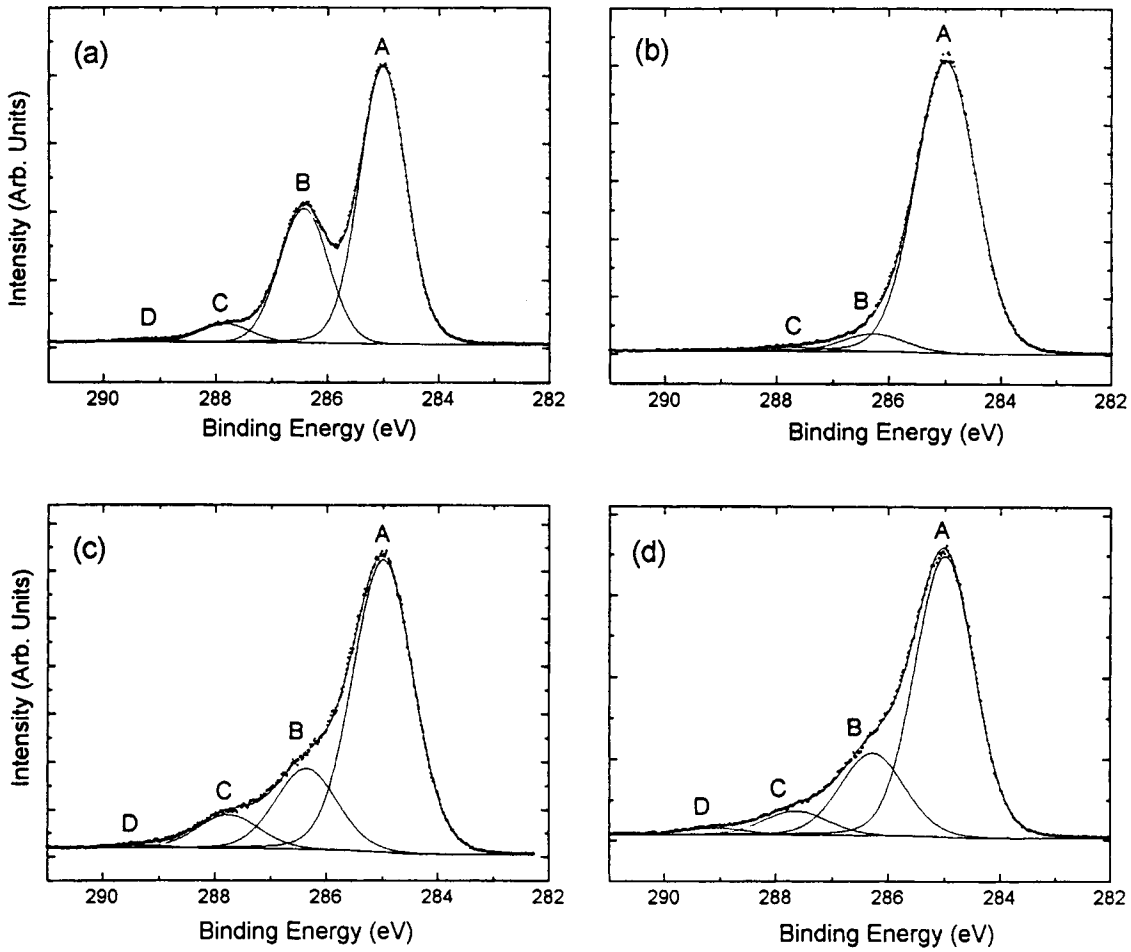

Figure 5 Simulation of the XPS C1s core level signals from (a) poly(allyl alcohol) obtained at 30 W (postdischarge region), (b) poly(allyl alcohol) obtained at 60 W (reactor), (c) poly(propargyl alcohol) obtained at 12 W (reactor), and (d) poly(1-propanol) obtained at 12 W (reactor).

and slit width: 0.75 mm) for which fwhm of 1.0, 1.0, and 1.1, respectively, were measured.

For power values above 30 W, films of poly(allyl alcohol) with a broader component A (fwhm = 1.26–1.30 eV) are formed (Table II). This broadening occurs in plasma conditions for which important oxygen elimination and ablation reactions have been observed (Figs. 2 and 3). It could result from the appearance of new types of unfunctionalized carbon atoms such as quaternary carbons. According to the

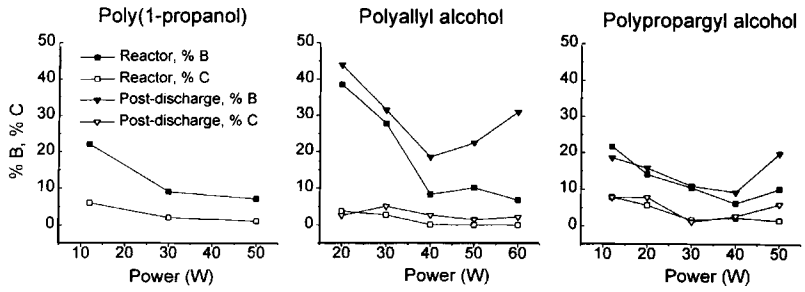

Figure 6 Percentages of B and C components obtained from the simulation of the C1s core level spectra of the polymers.

Table I Comparison of O/C (×100) Atomic Ratios with the Percentage of Carbon Bonded to Oxygen (B + C) (%) for Oxygen-rich Deposits

	Reactor		Postdischarge	
Power (W)	O/C (×100)	(B + C) (%)	O/C (×100)	(B + C) (%)
Poly(allyl alcohol)				
20	43	43	51	48
30	28	31	38	37
50	—	—	24	24
60	—	—	32	34
Poly(propargyl alcohol)				
12	27	29	28	26
20	18	19	21	23
50	—	—	28	26
Poly(1-propanol)				
12	20	28	—	—

Scienta ESCA 300 Database from Beamson and Briggs,[20] quaternary carbon atoms can be shifted up to 0.56 eV to lower binding energy from CH_2 type carbon atoms. This shift may explain the increase in fwhm from 1.0 to 1.3 eV. The appearance of unsaturated unprotonated carbon atoms which can have a binding energy lowered by 0.55 eV compared to CH_x carbon atoms could also be responsible for it.

Table II also shows that the fwhm of component A is high (1.27–1.43 eV) for poly(propargyl alcohol) and poly(1-propanol) synthesized in all plasma conditions. These broad components suggest again the presence of unprotonated carbon atoms (quaternary or unsaturated). As for these two polymers, more carbonyl functions have been detected by XPS, a contribution of the carbon atoms in the α position from the carbonyl groups (shifted by 0.38 eV to higher binding energy from the CH_2 carbon atoms) to the broadening of component A has to be taken into account.

IR Characterization

A comparison among the TIR spectra of poly(allyl alcohol), poly(propargyl alcohol), and their monomers is shown in Figure 8. Because of very low deposition rates for poly(1-propanol), TIR spectra of these polymers were not collected. Absorption bands due to the presence of alcohol and carbonyl functions

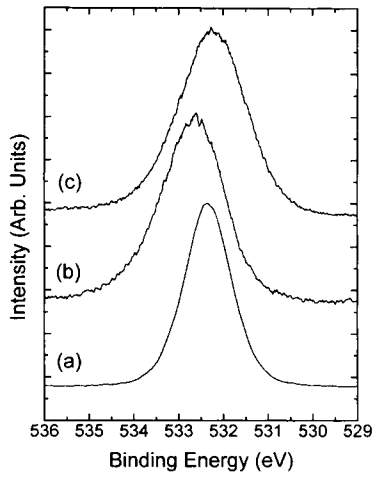

Figure 7 XPS O1s core level spectra of (a) poly(allyl alcohol) (20 W), (b) poly(1-propanol) (12 W), and (c) poly(propargyl alcohol) (20 W) obtained in the reactor.

are present on the spectra of the polymers. The OH stretching absorption bands (A1) are located between 3360 and 3480 cm^{-1} (Table III). This broad band appears at 3360 cm^{-1} for poly(allyl alcohol) deposited at low power (20 and 30 W) and is shifted to 3480 cm^{-1} for higher-power values. These different positions of the OH stretch band can be correlated to the oxygen content: For samples containing a great amount of hydroxyl functionalities, lower wave numbers of the OH stretch bands result probably from the formation of hydrogen bonding between the OH groups. Considering the position and width of the OH stretching absorption band for poly(propargyl alcohol), it seems that the tendency of hydrogen bonding is less pronounced for these polymers (Fig. 8) (Table III). For both polymers formed at low power, a C—O stretching absorption band of alcohol or ether functions is observed at 1060 cm^{-1} (I1).

Table II Full-width at Half-maximum (fwhm) of Component (A) Resulting from the Simulation of the C1s Core Levels of the Three Polymers Deposited in the Reactor

	Power (W)					
	12	20	30	40	50	60
Poly(allyl alcohol)	—	1.05	0.97	1.30	1.29	1.26
Poly(propargyl alcohol)	1.32	1.40	1.36	1.28	1.36	—
Poly(1-propanol)	1.27	—	1.40	—	1.43	—

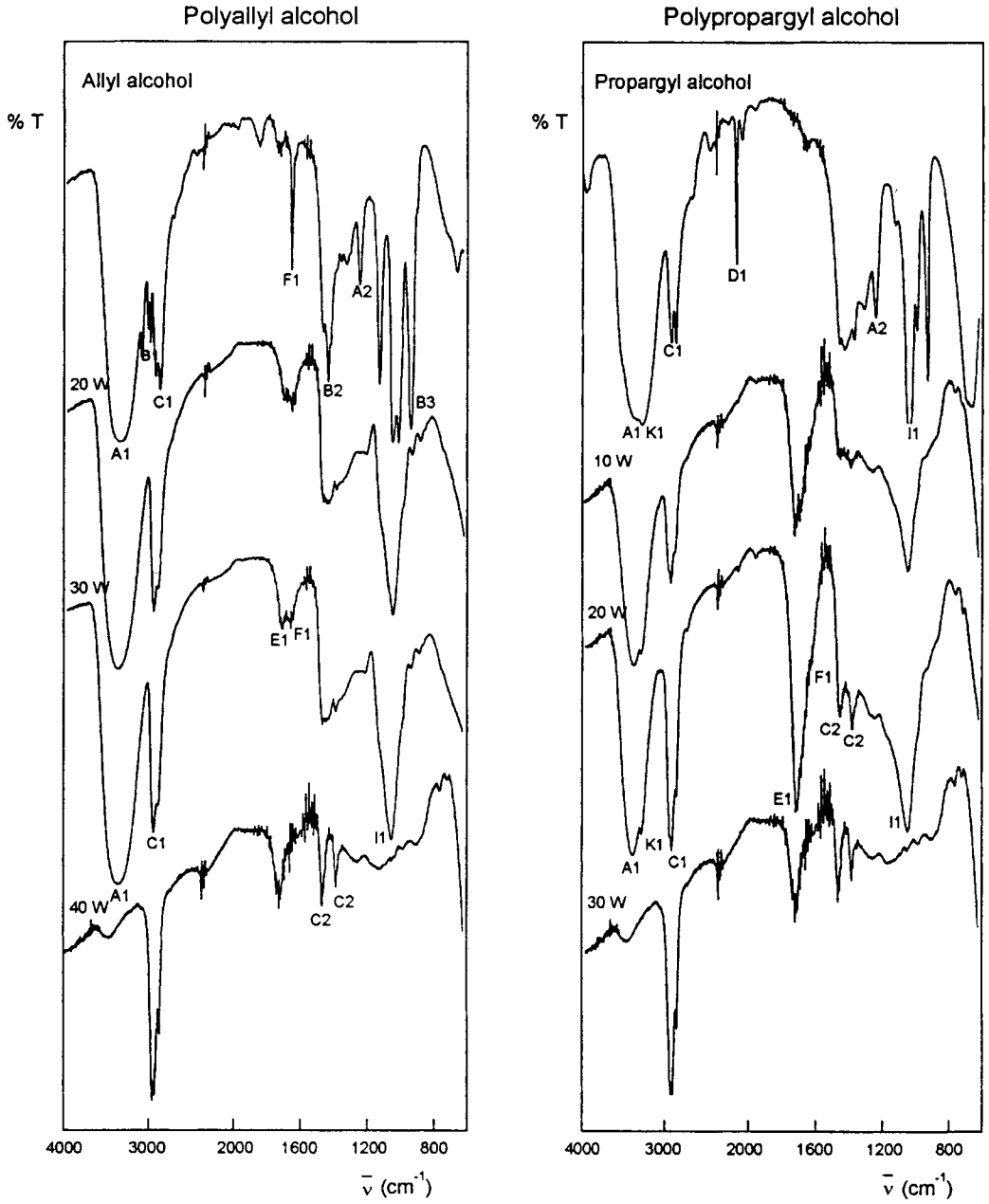

Figure 8 IR spectra of poly(allyl alcohol), poly(propargyl alcohol), and their monomers.

Table III Position of the TIR O—H Stretching Absorption Band (cm^{-1}) for the Polymers Obtained at Different Powers in the Reactor

		Power (W)					
		12	20	30	40	50	60
Poly(allyl alcohol)	$\bar{\nu}$ (cm^{-1})	—	3360	3360	3480	3480	3480
Poly(propargyl alcohol)	$\bar{\nu}$ (cm^{-1})	3400	3400	3480	3480	3480	—

Compared to the IR spectra of the monomers, a new peak appears at 1720 cm^{-1} (E1) (C=O stretching). It shows that carbonyl functions are formed during the polymerization process. The IR spectra evolutions vs. power agree with XPS results: Alcohol functions are mainly present in the films obtained from allyl alcohol at low power (20 and 30 W) (higher intensity of band A1). Moreover, the intensity of the carbonyl absorption band (E1) is more pronounced for poly(propargyl alcohol) in which more carbonyl functions have been detected by XPS.

Compared to the infrared spectra of pure monomers, it seems that some unsaturated carbon–carbon bonds remain in the films formed at low power. The stretching absorption band at 1660 cm^{-1} (F1) (C=C stretching) present on the spectrum of allyl alcohol appears also for both polymers. The presence of this band for poly(propargyl alcohol) shows that some triple C≡C bonds are partially converted into C=C double bonds in the plasma. However, the presence of the absorption band at 2300 cm^{-1} (K1) (C—H stretching from alkyne) on the IR spectra of this polymer shows that some triple bonds remain incorporated in the films.

The comparison of the IR spectra suggests that at high power these unsaturated groups are transformed into saturated ones: The intensity of peaks due to the presence of unsaturated carbon–carbon bonds decreases for higher-power values while aliphatic bend peaks increase (C2) (1470 and 1380 cm^{-1}).

Hydroxyl Derivatization with Trifluoroacetic Anhydride (TFAA)

Vapor-phase TFAA derivatization followed by XPS analysis is used to quantify the alcohol functions. The selectivity of TFAA toward hydroxyl groups has been tested by Chilkoti et al. and Sutherland et al. for different polymers containing various oxygen-functional groups.[8,21] These tests show that the reaction predominantly labels hydroxyl groups [TFAA reacts with nearly 100% of hydroxyl groups in poly(vinyl alcohol) without appreciably labeling polymers containing carbonyl, ether, or ester functions] and thus provide a semiquantitative comparison of the hydroxyl concentration for various oxygen-functionalized polymers. It has, however, been shown that TFAA is not entirely specific to the hydroxyl groups; it also reacts with epoxide groups.[22]

For our samples containing a great amount of alcohol functions, quantitative information on the functional groups (alcohol, ether, and carbonyl) is deduced from the simulation of the high-energy resolution core levels of samples analyzed before and after derivatization. If some epoxide groups are present in the samples, the concentration of hydroxyl groups can be overestimated by TFAA labeling.

Figure 9 shows the change of the core levels after derivatization of poly(allyl alcohol) deposited at 30 W in the reactor. The 25% fluorine detected in the derivatized sample confirm the presence of hydroxyl groups. The new peaks appearing on the C1s core level are attributed to carbons from the ester groups (E) (290.1 eV) and the $\underline{C}F_3$ carbon atoms (F) (293.3 eV). A new component (C) due to the ester group also modifies the O1s core-level shape.

The fluorine percentage of TFAA-derivatized poly(allyl alcohol) does not differ if the takeoff angle is modified (Table IV). This suggests that the reaction proceeds homogeneously over the full sampling depth analyzed by XPS. Therefore, quantitative information can be deduced from the analysis. The evolution of the fluorine percentage vs. power is the same as for the O/C ratio (Table V). The concentration of fluorine decreases vs. power for films deposited in the reactor while a decrease followed by an increase is observed for the ones obtained in the postdischarge position.

The evolution of the fluorine percentages is in agreement with XPS and IR results. Less fluorine is detected in oxygen-deficient polymers and in poly(propargyl alcohol) and poly(1-propanol) which contain more carbonyl functions and less carbon atoms single-bonded to oxygen than poly(allyl alcohol). For poly(1-propanol), this low fluorine percentage is also probably due to the presence of ether functions. These results show that the possible non-

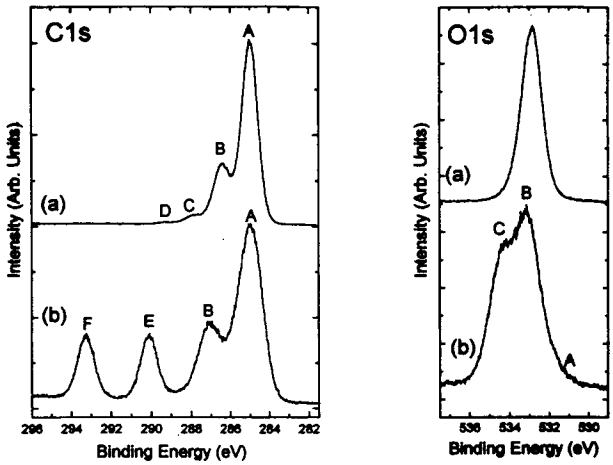

Figure 9 XPS C1s and O1s core levels spectra of poly(allyl alcohol) (30 W) obtained in the reactor (a) before and (b) after derivatization with TFAA.

Table IV Fluorine Percentages Obtained by XPS Analysis with Different Takeoff Angles (TOA) of TFAA-derivatized Poly(allyl alcohol) (30 W) (Reactor)

	TOA		
	90°	35°	15°
% F	26	25	26

specific adsorption of the labeling compound (without covalent coupling) observed by Chatelier et al. for some chemical derivatization reactions[23] is negligible here and that the reaction seems selective toward hydroxyl groups.

The percentages of the different oxygen-containing functionalities are determined by the simulation of the C1s core levels [Fig. 10(a)]. Assuming that the polymers contain alcohol, ether, carbonyl, epoxide, and ester or carboxylic acid functionalities, after the derivatization reaction, the ether, carbonyl, and ester groups remain unchanged. Therefore, the area of component C obtained from fitting the unlabeled spectrum was used in the fit of the labeled poly(allyl alcohol). This area ought not to be perturbed by labeling. The hydroxyl groups are transformed into ester functions and the carboxylic acid functionalities as well as the epoxide groups are also expected to react with TFAA.[8,22] Due to the very low intensity of component D on the C1s core level of the unlabeled polymer, the contribution of the reaction with the carboxylic acid functionalities is neglected.

The reaction of epoxide groups with TFAA has not been taken into account in the following quantification of the functional groups. If some epoxide groups are present in the samples, the calculated proportion of alcohol functions will be overestimated.

After reaction, the percentage of component E [290.1 eV; O$\underline{C}$(O)CF_3] is equivalent to the percentage of component F (293.3 eV; $\underline{C}F_3$). A value of 12% is obtained. The same amount of $\underline{C}$—O—C(O)CF_3 (12%) is also formed after reaction of the hydroxyl group with TFAA. Knowing the percentage of component B (286.9 eV; 20%) due to $\underline{C}$—O—C(O)CF_3 and $\underline{C}$—O—$\underline{C}$ carbon atoms, the percentage of $\underline{C}$—O—$\underline{C}$ (8%) is deduced. From these values, the proportion of the different oxygen functions is calculated. The polymer contains mainly alcohol functions (66%) but also some ether (22%) and carbonyl functions (12%).

To obtain a good fit, it was necessary to use larger fwhm for component A (fwhm = 1.43 eV) and component B (fwhm = 1.48 eV) than the one used for the other peaks in the spectrum (fwhm = 1.00–1.11 eV). These broadenings have been previously explained by Ameen who analyzed TFAA-derivatized poly(vinyl alcohol) and plasma-polymerized poly(allyl alcohol).[24] They result from the presence of additional components on the C1s core levels.

A similar fit as the one proposed by Ameen, with additional components, is shown in Figure 10(b). The high fwhm of the B component in the first fit [Fig. 10(a)] results from the presence of different $\underline{C}$—O carbon atoms shifted by 0.76 eV: Components B1 due to $\underline{C}$—O—$\underline{C}$ carbon atoms (8%; fwhm = 1.03 eV) and B2 resulting from $\underline{C}$—O—C(O)CF_3 carbon atoms (12%; fwhm = 1.01 eV) appear, respectively, at 286.69 and 287.45 eV in the second fit [Fig. 10(b)]. Knowing the stoichiometry of the reaction, to perform a good fit, the area of components F, E, and B2 have been fixed to be equivalent.

According to the authors, the broadening of component A after labeling results from the apparition of carbon atoms in β from the OC(O)CF_3 group ($\underline{C}$—C—OC(O)CF_3) shifted by 0.59 eV from unfunctionalized hydrocarbons. In our fit, component A2 (Eb = 285.63 eV; 21%; fwhm = 1.16 eV) is shifted by approximately the same value (0.63 eV) from component A1 (32%; fwhm = 1.18 eV; positioned at 285.0 eV). According to the measured area of com-

Table V Fluorine Percentages Obtained by XPS Analysis of the TFAA-derivatized Polymers (TOA = 35°)

	% F	
Power (W)	Reactor	Postdischarge
Poly(1-propanol)		
12	10	—
Poly(allyl alcohol)		
30	25	30
40	4	14
50	3	18
60	2	28
Poly(propargyl alcohol)		
12	17	18
20	15	13
30	4	8
40	7	10

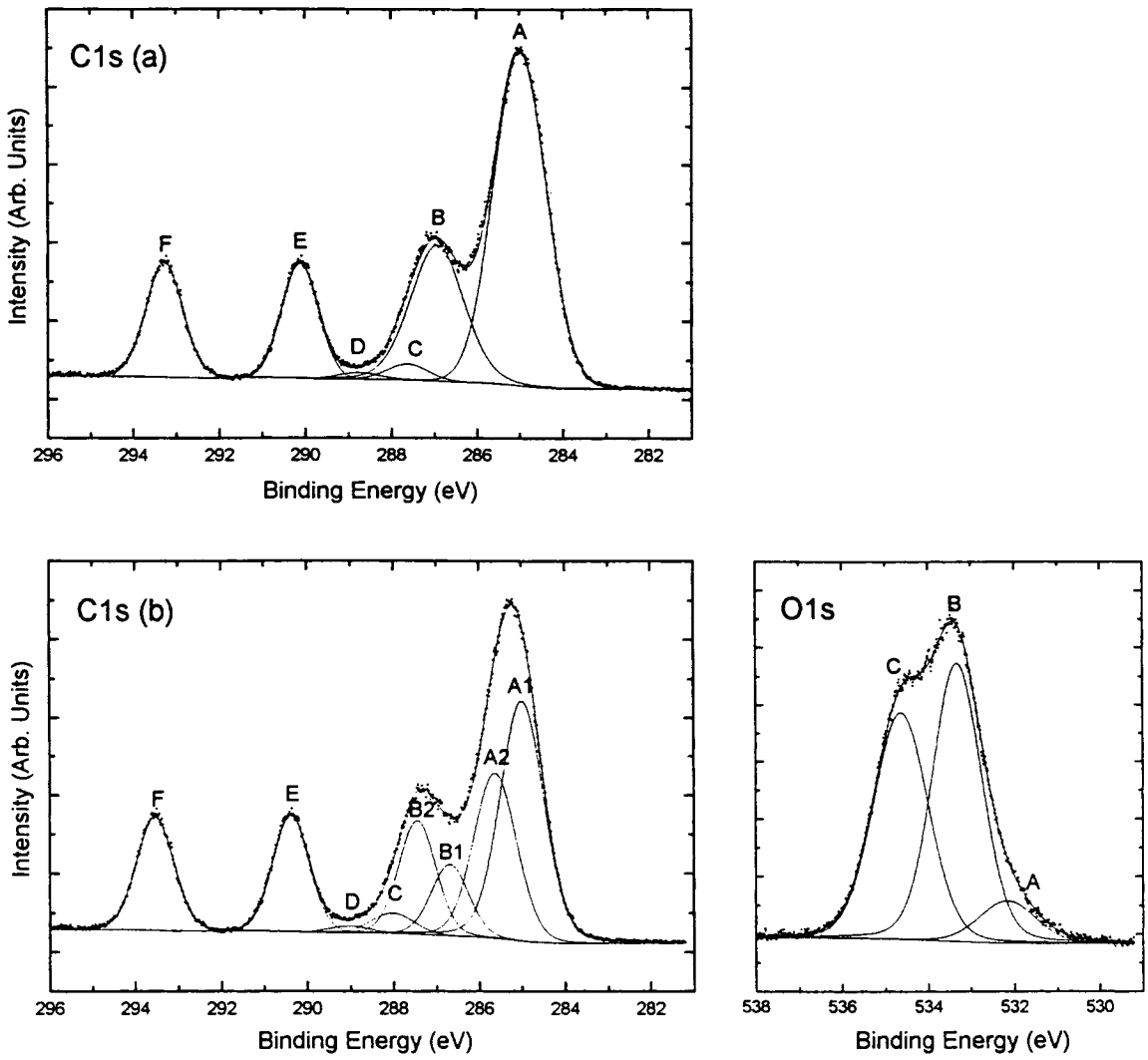

Figure 10 Simulation of the C1s and O1s signals of TFAA-derivatized poly(allyl alcohol) (30 W) obtained in the reactor.

ponent A2 (21%), which is higher than the areas of components B2, E, and F (12%), it seems that there are more carbon atoms in β from the $-OC(O)CF_3$ group than $OC(O)CF_3$ groups. This could result from the contribution of secondary or tertiary alcohol groups. This result differs from those of Ameen who assumed that the majority of alcohol exists as a primary alcohol group.

Compared to the first fit [Fig. 10(a)] where A was used as a reference and positioned at 285.0 eV, by performing a more precise simulation, the position of the assumed unfunctionalized hydrocarbon atoms has changed: A1 is now used as a reference. The calibrated binding energies of components C–F are approximately 0.3 eV higher than with the first one. The proportion of the different oxygen functions calculated from the second fit are similar to those deduced from the first fit.

Approximately the same values can also be deduced from the simulation of the O1s core level. The small contribution at 532.2 eV (A, 8%) is due to carbonyl functions while 40% of the O1s core level signal arises from one of the oxygen atoms from the ester group [$\underline{O}-C(O)CF_3$; component C; 534.6 eV]. The main component B at 533.3 eV (52%) includes the contributions of $O-C(\underline{O})CF_3$ (40%; same intensity as component C) and $C-\underline{O}-C$ (12%) oxygen atoms.

The proportion of functions was calculated by fitting the core levels for the other oxygen-rich polymers (Table VI). The degree of hydroxyl retention in poly(allyl alcohol) is very high: Up to 72% alcohol

Table VI Proportion of Functions for Oxygen-rich Deposits

Power (W)	Position	% Alcohol	% Carbonyl	% Ether
Poly(1-propanol)				
12	Reactor	24	26	50
Poly(allyl alcohol)				
30	Reactor	66	12	22
	Postdischarge	72	11	17
40	Postdischarge	53	16	31
50	Postdischarge	67	18	15
60	Postdischarge	66	8	26
Poly(propargyl alcohol)				
12	Reactor	36	34	30
20	Reactor	36	31	33
	Postdischarge	32	35	33
30	Postdischarge	41	19	40

functions are present in these polymers. Our results differ from those of Yuan and Marchant who also plasma-polymerized allyl alcohol and observed an important conversion of the hydroxyl groups into carbonyl functionalities.[3] To obtain hydroxyl groups, the authors reduced the carbonyl functions by an aqueous solution of borohydride. The concentration found for hydroxyl groups in the reduced films was about 30% of the oxygen content. Our plasma conditions seem more efficient as oxygen-rich polymers with a proportion of alcohol functions varying between 53 and 72% of the oxygen content could be obtained by direct polymerization of allyl alcohol.

Table VI shows that the hydroxyl conversion in the plasma is more pronounced for poly(1-propanol) and poly(propargyl alcohol): Alcohol, ether, and carbonyl functions are present in equivalent quantities in poly(propargyl alcohol) while poly(propyl alcohol) contains mainly ether functions (50%). This last result is in agreement with the comparison of the O/C (×100) ratio with the percentage of carbon atoms bonded to oxygen (B + C), which indicates the presence of ether functions or epoxide groups in this poly(1-propanol) (Table I).

On the other hand, as the oxygenated carbon percentage reflects the O/C ratio for poly(allyl alcohol) and poly(propargyl alcohol) (Table I), we deduced that component B originates mainly from carbon atoms bonded to alcohol functions and that very few ether functions or epoxide groups were present in these two polymers. Results from Table VI disagree with this deduction: The proportion of ether functions obtained from the derivatization reaction varies between 15 and 31% for poly(allyl alcohol) and between 30 and 40% for poly(propargyl alcohol). An overestimation of the ether percentage by labeling could result from an incomplete reaction of the alcohol functions with TFAA due to steric hindrance. Compared to model conventional polymers[8,21] on which the derivatization reactions are usually tested, our plasma polymers are more crosslinked or branched. It is possible that some alcohol functions cannot be reached by TFAA. In that case, the real concentration of alcohol functions in the polymers would then still be higher than the one calculated in Table VI.

The alcohol concentration can also be deduced from the F/O atomic ratios of the TFAA-derivatized samples. These calculations were performed for some oxygen-deficient films for which fitting the core levels cannot give quantitative values. Alcohol functions of 7 and 10% were, respectively, found in poly(allyl alcohol) (50 W) and poly(propargyl alcohol) (30 W) deposited in the reactor. These results show that in hard conditions the hydroxyl conversion in the plasma is more pronounced. Steric hindrance is also probably more important.

Elemental Analysis

The elemental composition of poly(propargyl alcohol) deposited in the reactor under different values of rf powers were obtained with a Heraeus CHN-O-Rapid elemental analyzer and compared to the XPS atomic ratios (Table VII). This technique allows the determination of the hydrogen percentages that cannot be reached by XPS. The values obtained by both analyses for the O/C ratios are relatively close. However, the percentages of oxygen found by elemental analysis are a little higher than those calculated from the XPS results. This could be due to some surface contamination by hydrocarbons, leading to an underestimation of the O/C atomic ratios by a surface-sensitive technique such as XPS. This can also result from some more oxygen contamination in the samples analyzed by elemental analysis. Prior to this analysis, the samples were immersed in water to remove the polymer from the substrate. The reaction of radicals with water could lead to the incorporation of oxygen in the films which would remain even after drying *in vacuo*. The higher oxygen content in the films analyzed by elemental analysis can also be due to a longer exposure time to the atmosphere before analysis.

By knowing the percentage of hydroxyl groups (sole oxygen atoms bonded to hydrogen) in the samples, it is possible to calculate the average number of hydrogen atoms bonded to a carbon atom (Table VII). Values of 1.21 and 1.23 are, respectively, found for the films formed at 20 and 30 W. Compared to the monomer for which one hydrogen atom is, on the average, bonded to one carbon atom, some hydrogenation occurs during the polymerization process. However, the hydrogen content in the films remains low ($CH_{1.21-1.23}$). This can result from the presence of unsaturations (C=C or C≡C bonds) in the films that have been detected by IR spectroscopy. The presence of tertiary or quaternary carbon atoms (detected by XPS) is also probably responsible for it.

HREELS Characterization

The HREEL spectrum of poly(propargyl alcohol) obtained at 15 W in the reactor is shown in Figure 11. It has a resolution of 21 meV (measured as the fwhm of the elastic peak). Despite the relatively poor resolution of this spectrum compared to the IR spectrum, some bands or shoulders are clearly visible and can easily be identified. Their positions are approximately the same as for the bulk infrared spectrum of the polymer (Fig. 8). The bands due to hydrocarbon groups which are always present on the HREEL spectra of polymers[25] appear at 2960 cm^{-1} (C—H stretching) and 1360 cm^{-1} (C—H bending). Because of the very high sensitivity of this technique to the extreme surface, the presence of a peak at 3400 cm^{-1} (O—H stretching) shows that alcohol functions are present in the top 0–20 Å of the polymer. The C—O stretching vibration is being observed at 1080 cm^{-1}. The shoulder at 1720 cm^{-1} is attributed to C=O or C=C stretching vibrations.

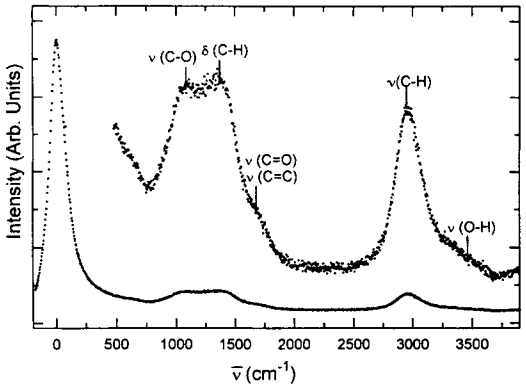

Figure 11 HREEL spectrum of poly(propargyl alcohol) obtained at 15 W in the reactor.

The comparison of the HREEL spectra of poly(allyl alcohol) (20 W) and poly(propargyl alcohol) (15 W) deposited in the reactor is shown in Figure 12. Although more alcohol functions were detected by XPS and TIR spectroscopy in poly(allyl alcohol) than in poly(propargyl alcohol), the C—O stretching absorption band (1080 cm^{-1}) is of lower intensity while the OH stretching absorption band (3400 cm^{-1}) is not present on the HREEL spectrum of poly(allyl alcohol).

This could be due to a different chemical composition at the extreme surface compared to the bulk polymer. For poly(allyl alcohol) deposited at low power, formation of hydrogen bonding between OH groups were deduced from the position and broadening of the infrared OH stretching absorption band. Moreover, a very low content of unprotonated carbon atoms (quaternary or unsaturated) are present in the films. We can therefore suppose that because there is enough chain mobility and because of the tendency of hydrogen bonding the hydroxyl groups are pointed mainly to the bulk of the films: Hydro-

Table VII Atomic Ratios Obtained by Elemental and XPS Analysis of Poly(propargyl alcohol) Obtained in the Reactor

Power (W)	% OH	Type of Analysis		Elemental Composition		
Monomer	100	Theoretical value	C_1	H_1	$(OH)_{0.33}$	
20	36	XPS	C_1		$O_{0.18}$	
			C_1	H_x	$O_{0.12}$	$(OH)_{0.06}$
		Elemental	C_1	$H_{1.27}$	$O_{0.23}$	
			C_1	$H_{1.21}$	$O_{0.17}$	$(OH)_{0.06}$
30	10	XPS	C_1		$O_{0.07}$	
			C_1	H_x	$O_{0.06}$	$(OH)_{0.007}$
		Elemental	C_1	$H_{1.24}$	$O_{0.11}$	
			C_1	$H_{1.23}$	$O_{0.10}$	$(OH)_{0.007}$

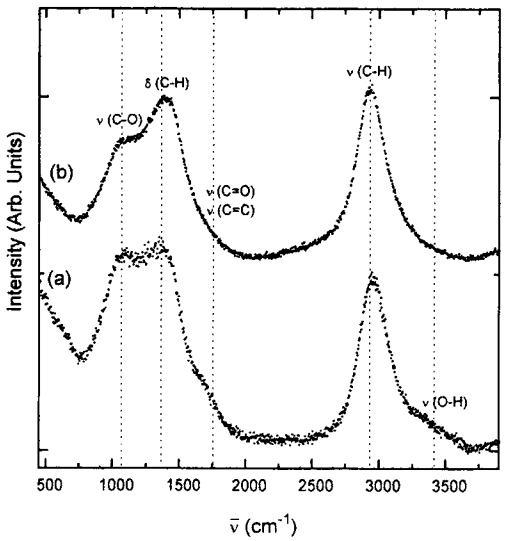

Figure 12 Comparison of the HREEL spectra of (a) poly(propargyl alcohol) (15 W) and (b) poly(allyl alcohol) (20 W) obtained in the reactor.

carbon groups are present mainly at the extreme surface. The disappearance of the hydroxyl groups from the extreme surface would explain the absence of the OH stretching absorption band on the HREEL spectrum of poly(allyl alcohol).

For poly(propargyl alcohol), the chain mobility is probably reduced because of the higher degree of crosslinking of this polymer (higher concentration of unprotonated carbon atoms). Moreover, as the tendency of hydrogen bonding is less pronounced, the hydroxyl groups remain probably at the extreme surface of the polymer. This could explain why the intensities of the O—H and C—O stretching absorption bands are higher for the polymer containing fewer alcohol functions.

The lower intensity of the C=O or C=C stretching absorption band (1720 cm^{-1}) for poly(allyl alcohol) compared to poly(propargyl alcohol) is well in agreement with the XPS and TIR results as less carbonyl functions and C=C bonds have been detected in poly(allyl alcohol).

DISCUSSION

This detailed characterization shows that the three selected monomers containing alcohol functions lead to the formation of polymers with very different chemical structures and functional groups. This suggests different polymerization mechanisms, depending on the degree of unsaturation of the starting material. The composition of the polymers is also very dependent on the plasma conditions.

XPS results show that the plasma polymerization of the saturated monomer (1-propanol) leads to the formation of oxygen-deficient films. For the unsaturated monomers (allyl alcohol and propargyl alcohol), elimination of oxygen fragments responsible for ablation have been observed in the reactor at high power. However, for these two monomers, at low power for the two positions or at high power in the postdischarge region, the polymerization proceeds with less fragmentation of the precursor and oxygen-rich polymers are deposited. The behaviors of the different monomers studied, in relation to the chemical structure of the polymers formed, are discussed here below:

Poly(allyl alcohol)

The detailed characterization of poly(allyl alcohol) obtained in soft conditions suggests that the double bond is involved in the deposition mechanism: allyl alcohol polymerizes more rapidly than does the saturated monomer. Moreover, the degree of hydroxyl retention in these films is relatively high; a proportion of alcohol functions between 53 and 72% of the oxygen content has been deduced from the simulation of the core levels of the TFAA-derivatized samples. The low fwhm of component A resulting from the simulation of the C1s core levels of poly(allyl alcohol) suggests a very low content of unprotonated carbon atoms (quaternary or unsaturated) in this polymer. This indicates that the degree of crosslinking of poly(allyl alcohol) is not very important and that relatively little bond breaking occurs during the polymerization process. This seems to confirm that the polymerization proceeds via the double bond. However, the simulation of the C1s core level of the TFAA-derivatized poly(allyl alcohol) reveals that there are more carbon atoms in β from the —OC(O)CF_3 groups than the OC(O)CF_3 groups. This has been explained by the contribution of secondary or tertiary alcohol groups and results therefore from some C—H bond breaking in the plasma leading to chain branching reactions. Despite these chain branching reactions, the chain mobility in the films seems to be sufficient to allow the formation of hydrogen bonding between alcohol functions. Their orientation into the bulk of the films and disappearance from the extreme surface have been detected by HREELS.

The polymerization mechanism of allyl alcohol is very dependent on the plasma conditions: In the reactor at high power, important ablation re-

actions and oxygen elimination were observed. Moreover, the hydroxyl conversion is more pronounced in these conditions: Less than 10% alcohol functions were found in the polymers. In addition to that, the appearance of numerous unprotonated carbon atoms (quaternary or unsaturated) shows that important crosslinking reactions occur in such hard conditions.

Poly(propargyl alcohol)

Although the higher deposition rates of this monomer compared to the other monomers suggest an important contribution of the triple bond to the polymerization mechanism, even in soft conditions, the degree of hydroxyl conversion in the plasma is relatively high: Alcohol, ether, and carbonyl functions are present in equivalent quantities in the films. In addition to that, results from the simulation of the C1s core level suggest the presence of numerous unprotonated carbon atoms (quaternary or unsaturated). This is supported by the relatively low hydrogen content detected by elemental analysis, which is an indication of crosslinking of the samples or of the presence of unsaturations. Unsaturated carbon–carbon bonds have also been detected by infrared analysis.

Because of the higher degree of crosslinking of this polymer compared to poly(allyl alcohol), the chain mobility is reduced. This higher film rigidity as well as the lower tendency to form hydrogen bonds explain why more alcohol functions have been detected by HREELS at the extreme surface of this polymer than in poly(allyl alcohol) although less hydroxyl groups are found in the bulk poly(propargyl alcohol).

Poly(1-propanol)

Much bond breaking occurs during the polymerization of this saturated monomer which deposits very slowly. Important oxygen elimination and hydroxyl group conversion (50% ether, 26% carbonyl, and 24% alcohol functions) were detected by XPS and derivatization. Moreover, the samples are probably highly crosslinked; they contain many unprotonated carbon atoms.

CONCLUSION

The study of the surface chemistry of films created from monomers containing alcohol functions, differing by the degree of unsaturation (1-propanol, allyl alcohol, and propargyl alcohol), demonstrates the tendency of fragmentation of these precursors. XPS results show that in the reactor at high power elimination of oxygen fragments responsible for ablation takes place during the polymerization process. However, oxygen-rich polymers can be deposited from the unsaturated monomers at low power for the two positions or at high power in the post-discharge region.

Detailed structural information on the chemical structure and content of functional groups has been obtained by high-energy resolution XPS, IR, HREELS, elemental analysis, and chemical derivatization with TFAA. Allyl alcohol is the most effective precursor to produce polymers containing alcohol functions. In soft conditions, the double bond of this monomer seems to be involved in the polymerization mechanism, leading to the formation of polymers with a relatively low degree of crosslinking and high hydroxyl content (proportion of alcohol functions varying between 53 and 73%). However, the presence of secondary or tertiary alcohol in these films has suggested some chain branching reactions. Despite these branching reactions, the chain mobility remains high: The alcohol functions tend to point inside of the polymer.

The hydroxyl conversion in the plasma is more pronounced for poly(1-propanol) and poly(propargyl alcohol). In soft conditions, alcohol, ether, and carbonyl functions are present in equivalent quantities in poly(propargyl alcohol) while poly(1-propanol) contains mainly ether functions (50%). Moreover, these two polymers are crosslinked: They contain unprotonated carbon atoms (quaternary or unsaturated). Although fewer hydroxyl groups are present in poly(propargyl alcohol) compared to poly(allyl alcohol), more alcohol functions have been detected by HREELS at the extreme surface. This has been explained by the lower chain mobility as well as a lower tendency of hydrogen bonding between alcohol functions for poly(propargyl alcohol).

For all polymers, a large degree of hydroxyl conversion has been observed under hard conditions: Less than 10% alcohol functions were left in the polymers deposited at high power in the reactor, which were highly crosslinked.

The authors are grateful to M. Vermeersch and L.-M. Yu for assistance in the acquisition of the HREEL spectra. We also thank Solvay for performing the elemental analysis.

REFERENCES

1. K. Hozumi, *Pure Appl. Chem.*, **60,** 697–702 (1988).
2. D. J. Hook, T. G. Vargo, J. A. Gardella, Jr., K. S. Litwiler, and F. V. Bright, *Langmuir,* **7,** 142–151 (1991).
3. S. Yuan and R. E. Marchant, Polymer preprints from the American Chemical Society Meeting, Denver, Colorado, 1993, Vol. 34, pp. 665–666.
4. F. Fally, C. Doneux, J. Riga, and J. J. Verbist, *J. Appl. Polym. Sci.,* **56,** 597–614 (1995).
5. Y. Nakayama, T. Takahagi, F. Soeda, K. Hatada, S. Nagaoka, J. Suzuki, and A. Ishitani, *J. Polym. Sci. Polym. Chem. Ed.,* **26,** 559–572 (1988).
6. Q. I. Wang, S. Kaliaguine, and A. Ait-Kadi, *J. Appl. Polym. Sci.,* **48,** 121–136 (1993).
7. T. J. Vargo, E. J. Bekos, Y. S. Kim, J. P. Ranieri, R. Bellamkonda, P. Aebischer, D. E. Margevich, P. M. Thompson, F. V. Bright, and J. A. Gardella, Jr., *J. Biomed. Mater. Res.,* **29,** 767–779 (1995).
8. A. Chilkoti, B. D. Ratner, and D. Briggs, *Chem. Mater.,* **3,** 51–61 (1991).
9. D. L. Cho, P. M. Claesson, C.-G. Gölander, and K. Johansson, *J. Appl. Polym. Sci.,* **41,** 1373–1390 (1990).
10. Q. Zhao, Y. Zhu, Y. Xu, Y. Yao, and X. Liu, *J. Appl. Polym. Sci.,* **44,** 1853–1859 (1992).
11. F. Denes, A. M. Samardi, C. E. C. A. Hop, and R. A. Young, Polymer preprints from the American Chemical Society Meeting, Denver, Colorado, 1993, Vol. 34, pp. 685–686.
12. F. Fally, I. Virlet, J. Riga, and J. J. Verbist, *J. Appl. Polym. Sci. Appl. Polym. Symp.,* **54,** 41–53 (1994).
13. G. Beamson, D. Briggs, S. F. Davies, I. W. Fletcher, D. T. Clark, J. Howard, U. Gelius, B. Wannberg, and P. Balzer, *Surf. Interface Anal.,* **15,** 541–549 (1990).
14. D. S. Everhart and C. N. Reilley, *Anal. Chem.,* **53,** 665–676 (1981).
15. M. P. Seah and W. A. Dench, *Surf. Interface Anal.,* **1,** 2–11 (1979).
16. G. P. López and B. D. Ratner, *Langmuir,* **7,** 766–773 (1991).
17. M. Liehr, P. A. Thiry, J. J. Pireaux, and R. Caudano, *Phys. Rev. B,* **33,** 5682–5697 (1986).
18. S. Nowak, J. A. M. Van der Mullen, B. Van der Sijde, and D. C. Schram, *J. Quant. Spectrosc. Radiat. Transfer,* **41,** 177–186 (1989).
19. H. Yasuda, *Plasma Polymerization,* Academic Press, Orlando, FL, 1985, 178–195.
20. G. Beamson and D. Briggs, *High Resolution XPS of Organic Polymers,* Wiley, Chichester, 1992, 182–224.
21. I. Sutherland, E. Sheng, D. M. Brewis, and R. J. Heath, *J. Mater. Chem.,* **4,** 683–687 (1994).
22. A. Chilkoti and B. D. Ratner, *Surf. Interface Anal.,* **17,** 567–574 (1991).
23. R. C. Chatelier, T. R. Gengenbach, and H. J. Griesser, Polymer preprints from the American Chemical Society Meeting, Denver, Colorado, 1993, Vol. 34, pp. 683–684.
24. A. P. Ameen, R. J. Ward, R. D. Short, G. Beamson, and D. Briggs, *Polymer,* **34,** 1795–1799 (1993).
25. Y. Novis, N. Degosserie, M. Chtaïb, J. J. Pireaux, R. Caudano, P. Lutgen, and G. Feyder, *J. Adhes. Sci. Technol.,* **7,** 699–717 (1993).

Received March 7, 1995
Accepted August 15, 1995